Molecular Biology of the Cell
Vol. 21, 1991–2000, June 15, 2010

Altered Lipid Droplet Dynamics in Hepatocytes Lacking Triacylglycerol Hydrolase Expression

Huajin Wang,*† Enhui Wei,†‡ Ariel D. Quiroga,†‡ Xuejin Sun,§ Nicolas Touret,‖ and Richard Lehner,*†‡

Departments of *Cell Biology, ‡Pediatrics and ‖Biochemistry, and †Group on Molecular and Cell Biology of Lipids, University of Alberta, Edmonton, Alberta T6G 2S2, Canada; and §Department of Oncology, University of Alberta, Cross Cancer Institute, Edmonton, Alberta T6G 1Z2, Canada

Submitted May 4, 2009; Revised April 8, 2010; Accepted April 12, 2010
Monitoring Editor: Robert G. Parton

Lipid droplets (LDs) form from the endoplasmic reticulum (ER) and grow in size by obtaining triacylglycerols (TG). Triacylglycerol hydrolase (TGH), a lipase residing in the ER, is involved in the mobilization of TG stored in LDs for the secretion of very-low-density lipoproteins. In this study, we investigated TGH-mediated changes in cytosolic LD dynamics. We have found that TGH deficiency resulted in decreased size and increased number of LDs in hepatocytes. Using fluorescent fatty acid analogues to trace LD formation, we observed that TGH deficiency did not affect the formation of nascent LDs on the ER. However, the rate of lipid transfer into preformed LDs was significantly slower in the absence of TGH. Absence of TGH expression resulted in increased levels of membrane diacylglycerol and augmented phospholipid synthesis, which may be responsible for the delayed lipid transfer. Therefore, altered maturation (growth) rather than nascent formation (de novo synthesis) may be responsible for the observed morphological changes of LDs in TGH-deficient hepatocytes.

INTRODUCTION

Lipid droplets (LDs), also known as lipid bodies, are lipid storage organelles in essentially all organisms. They consist of a neutral lipid core surrounded by a monolayer of amphipathic lipids (phospholipids and cholesterol) and LD-associated proteins (Martin and Parton, 2006; Olofsson *et al*., 2008). Instead of the conventional perception of being inert storage particles, LDs have been recently recognized as highly dynamic, *bona fide* organelles that play central roles in energy metabolism (Martin and Parton, 2006; Brasaemle, 2007). Abnormalities in LD dynamics are implicated in human diseases such as obesity, cardiovascular disease, type 2 diabetes, and fatty liver.

The hydrophobic core of LDs contains lipid esters, mainly triacylglycerol (TG) and cholesteryl ester. In conditions when intracellular fatty acids (FA) are in excess, cells rapidly form TG that is deposited in LDs. This response is considered to serve as protection against lipotoxic effects of free FA (Gibbons *et al*., 2000). It is generally believed that LD biogenesis in eukaryotes initiates from the endoplasmic reticulum (ER) where TG biosynthesis takes place. It has been proposed that newly synthesized TG accumulates between the two leaflets of the ER bilayer, forming a lens-like structure, which will further separate from the ER and form an independent nascent LD through budding or "hatching" (Murphy and Vance, 1999; Fujimoto *et al*., 2008). However, little is known about the mechanism by which nascent LDs accrue additional TG and grow in size after nascent formation. Some studies suggest that LDs remain in contact with the ER, whereas other reports argue that LDs probably pinch off from the ER and become independent structures (Brasaemle, 2007; Walther and Farese, 2009). It was recently reported that in COS7 cells and adipocytes acyl-CoA:diacylglycerol acyltransferase-2 was present in proximity with LDs, suggesting that TG may be transferred into the LD core via a tight ER–LD association (Kuerschner *et al*., 2008).

The liver is a central organ for lipid metabolism not only because of its large capacity for neutral lipids storage but also because hepatocytes are specialized cells responsible for the secretion of TG into circulation in the form of very-low-density lipoprotein (VLDL) (for review, see Gibbons *et al*., 2000). In lipoprotein-secreting cells (hepatocytes and enterocytes) at least three types of LDs exist: cytosolic LDs, ER luminal apoB-free LDs, and apoB-containing VLDL precursor particles (Olofsson *et al*., 2000; Shelness and Sellers, 2001). Lipolysis of TG stored in LDs provides substrates for VLDL-TG synthesis (Wiggins and Gibbons, 1992; Yang *et al*., 1996; Lankester *et al*., 1998). LDs undergo lipolysis very rapidly but only a small portion of the released FA are integrated into VLDL and secreted; the majority is recycled back to LDs via a futile cycle (Wiggins and Gibbons, 1992; Gibbons and Wiggins, 1995). Lipases responsible for the hydrolysis of stored hepatic TG would be predicted to play important roles in the turnover of both cytosolic LDs and luminal LDs. However, the identities of lipases that perform these functions in the liver are not yet known with certainty. Hormone-sensitive lipase (HSL) is a major cytosolic lipase in adipocytes, but it is generally considered to be absent from

This article was published online ahead of print in *MBoC in Press* (http://www.molbiolcell.org/cgi/doi/10.1091/mbc.E09–05–0364) on April 21, 2010.

Address correspondence to: Richard Lehner (richard.lehner@ualberta.ca).

Abbreviations used: ADRP, adipose differentiation-related protein; ATGL, adipose triglyceride lipase; BSA, bovine serum albumin; DG, diacylglycerol; ER, endoplasmic reticulum; FA, fatty acids; HSL, hormone-sensitive lipase; KO, knockout; LD, lipid droplet; McA, McArdle-RH7777; OA, oleic acid; PEMT, phosphatidylethanolamine N-methyltransferase; PC, phosphatidylcholine; PL, phospholipids; TG, triacylglycerol; TGH, triacylglycerol hydrolase; VLDL, very-low density lipoprotein; WT, wild-type.

the liver (Holm *et al*., 1987). Another recently identified cytosolic lipase that catalyzes the initial step in TG hydrolysis, adipose triglyceride lipase (ATGL), is only expressed at a very low level in the liver (Zimmermann *et al*., 2004). In addition, overexpression of either ATGL or HSL in the liver did not lead to increased provision of lipids for VLDL assembly but rather promoted delivery of released FA to mitochondrial oxidation (Reid *et al*., 2008). These results suggested that other lipases function in the mobilization of LDs to provide substrates for VLDL assembly and that the intracellular location of lipases might determine the fate of the lipolytic products. One candidate lipase that has been shown to participate in the mobilization of TG for VLDL assembly is an ER luminal carboxylesterase, also termed triacylglycerol hydrolase (TGH) (Lehner and Verger, 1997; Lehner and Vance, 1999; Gilham *et al*., 2003; Dolinsky *et al*., 2004; Gilham and Lehner, 2004; Wei *et al*., 2007a, 2010). Ectopic expression of TGH in McArdlle-RH7777 (McA) hepatoma cells led to decreased levels of cytosolic TG, suggesting that this ER-localized lipase also participates in the turnover of cytosolic LD-TG (Wang *et al*., 2007). In the current research, we investigated the mechanism by which TGH affects cytosolic LD dynamics.

MATERIALS AND METHODS

Animals

All animal procedures were approved by the University of Alberta's Animal Care and Use Committee and were in accordance with guidelines of the Canadian Council on Animal Care. All wild-type (WT) or TGH knockout (TGH KO) mice used in this study were 3- to 4-mo-old females maintained on chow diet (PicoLab Rodent Diet 20; LabDiet, Richmond, IN). Unless otherwise stated, all mice were fasted for 4 h before experiments.

Materials

DMEM, fetal bovine serum (FBS), and horse serum were purchased from Invitrogen Canada (Burlington, ON, Canada). Bovine serum albumin, essentially fatty acid free (BSA) and Complete protease inhibitor cocktail tablets were from Roche Diagnostics (Laval, QC, Canada). Anti-mouse TGH antibodies were generated in our laboratory (Wang *et al*., 2007). Anti-protein disulfide isomerase (PDI) and anti-calnexin polyclonal antibodies were from AKELA Pharma (Montreal, QC, Canada). Anti-microsomal triglyceride transfer protein monoclonal antibodies were from BD Biosciences Canada (Mississauga, ON, Canada). Rabbit anti-adipose differentiation-related protein (ADRP) antibodies were a kind gift from Dr. C. Londos (National Institutes of Health, Bethesda, MD), rabbit anti-TIP47 antibodies were a generous gift from Dr. C. Sztalryd (University of Maryland, College Park, MD), and rabbit anti-phosphatidylethanolamine-*N*-methyltransferase (PEMT) antibodies were provided by Dr. D. Vance (University of Alberta, Edmonton, AB, Canada). Horseradish peroxidase-conjugated secondary antibodies were from Pierce Chemical (Rockford, IL). Full-range rainbow protein molecular weight marker and enhanced chemiluminescence immunoblotting reagents were obtained from GE Healthcare Canada (Baie d'Urfe, QC, Canada). Bradford protein assay reagent was from Bio-Rad Laboratories Canada (Mississauga, ON, Canada). ProLong Antifade kit, Alexa 488-conjugated goat-anti-rabbit immunoglobulin G, Bodipy 493/503, Bodipy FL C_{12}, and Bodipy 558/568 C_{12} were purchased from Invitrogen (Carlsbad, CA). QTB fatty acid uptake assay kit was purchased from Molecular Devices (Sunnyvale, CA). All other reagents were of analytical grade or higher.

Subcellular Fractionation

Subcellular fractions for protein and lipid mass analysis were isolated from the livers or hepatocytes of WT or TGH KO mice as described previously (Wang *et al*., 2007). The floating lipid layers (crude fat cake) after 106,000 $\times$ *g* 1-h spin of postmitochondrial supernatants were collected. The crude fat cake layer was then overlaid with Tris-buffered saline (TBS) and subjected to ultracentrifugation at 106,000 $\times$ *g* for 1 h to float cytosolic LDs. Cytosolic LDs were collected and suspended in TBS. Protein concentration of each fraction was determined by Bradford method.

TGH-enhanced Green Fluorescent Protein (EGFP) Construct

The TGH-EGFP construct was generated by inserting the EGFP coding sequence into the TGH cDNA immediately before the region encoding the C-terminal "HIEL" ER retrieval sequence (Gilham *et al*., 2005).

Preparation of Primary Mouse Hepatocytes

Primary mouse hepatocytes were isolated by collagenase perfusion of the livers from WT and TGH KO mice and were plated on collagen-coated coverslips in six-well dishes at 2.0 $\times$ 10^5 cells/dish. Hepatocytes were maintained in DMEM supplemented with 10% FBS at 37°C in humidified air containing 5% CO_2.

Transfection of Hepatocytes

Hepatocytes were transfected using the Targefect-Hepatocytes reagent (Targeting Systems, El Cajon, CA) following the user's manual. In brief, hepatocytes plated on collagen-coated coverslips at ~70% confluence were maintained in DMEM containing 10% FBS. To transfect cells in 24-well dishes, 0.8 μg of plasmid DNA encoding TGH-EGFP was mixed with 250 μl of DMEM. At the same time, 1.5 μl of Targefect reagent and 3 μl of enhancer (Virofect) were mixed with 250 μl of DMEM. The mixtures were then mixed and incubated for 20 min at 37°C to yield the transfection complex. Cells were incubated with the transfection complex for 4 h in serum-free media, and then the media were replaced with DMEM containing 10% FBS and maintained for at least 14 h before visualization of TGH-EGFP fluorescence by a fluorescent microscope.

Detection of LDs by Fluorescent Microscopy

To visualize LDs, freshly isolated hepatocytes were grown on collagen-coated coverslips for 4 h, washed three times with phosphate-buffered saline (PBS), followed by incubation with 2 μg/ml Bodipy 493/503 in PBS. To visualize LD formation, cells grown on collagen-coated coverslips were washed with PBS and incubated overnight in DMEM containing 0.4 mM oleic acid (OA) complexed to 0.5% BSA (essentially fatty acid free) and 6 μM Bodipy FL C_{12} or Bodipy 558/568 C_{12}. For confocal imaging of preformed versus newly made LDs containing fluorescent lipids, cells were incubated with OA/BSA media containing Bodipy FL C_{12} overnight (preformed LDs) and then washed with PBS and incubated with OA/BSA containing Bodipy 558/568 C_{12} for 15 min, 30 min, 1 h, or 4 h (newly made LDs). Labeling of cells with fluorescent FA was stopped by washing cells with PBS and fixed immediately with 4% paraformaldehyde in PBS. For live-cell imaging, cells were first incubated with Bodipy 558/568 C_{12} overnight to fluorescently label preformed LDs. Nascent LDs were labeled by QTB FA uptake reagent (containing Bodipy FL C_{12}) reconstituted in 10 ml of DMEM containing OA/BSA immediately before image acquisition.

Immunofluorescence Staining

Hepatocytes grown on collagen-coated coverslips were incubated with DMEM containing OA/BSA for 4 h or overnight to build up neutral lipid stores before immunostaining. For colocalization with nascent LDs, cells were incubated with OA/BSA containing Bodipy 558/568 C_{12} for 15 min before staining. Cells were rinsed with PBS, fixed with 4% paraformaldehyde and 0.025% glutaraldehyde in PBS, followed by background quenching with 50 mM NH_4Cl in PBS. Cells were then permeabilized with 0.05% saponin in PBS for 15 min and blocked with 3% normal goat serum in PBS. Anti-ADRP and TIP47 antibodies were used at 1:200 dilution with PBS containing 3% BSA for 1 h at 37°C.

Confocal Fluorescence Scanning Microscopy

Images of fixed cells were collected with a confocal laser scanning microscope (LSM510, software version 3.2'; Carl Zeiss, Jena, Germany) mounted on an Axiovert 100M inverted microscope (Carl Zeiss), with a Plan-Apochromat differential interference contrast (DIC) 63$\times$ (1.40 numerical aperture [NA]) objective. To image Bodipy 493/503 staining, the 488 nm laser line was used and signals were collected with a long pass filter 505 nm. For dual-color images, the 488 nm laser line was used to image Bodipy FL C_{12} and the 543 nm laser line was used to image Bodipy 558/568 C_{12}. Signals were collected with a band pass 500–530 nm filter-IR blocking and a long pass 560 nm filter, respectively. Quantification of LD number and sizes was done with MetaMorph, version 7.5 (Molecular Devices).

Time-Lapse Confocal Microscopy

Cells grown on coverslips were mounted onto an adaptator (Chamlide, Seoul, Korea) and placed in an environment chamber thermostated at 37°C and supplied with 5% CO_2. Confocal microscopy was performed on a spinning-disk microscope (WaveFx from Quorum Technologies, Guelph, ON, Canada) set up on an IX-81 inverted stand (Olympus, Markham, ON, Canada). Images were acquired through a 60$\times$ objective (1.42 NA), with an electron multiplying charge-coupled device camera (Hamamatsu, Hamamatsu City, Shizuoka, Japan). The fluorescent FA analogues Bodipy FL C_{12} and Bodipy 558/568 C_{12} were successively excited by a 491 nm (green fluorescent protein [GFP] channel) and a 543 nm (Cy3 channel) laser line (Spectral Applied Research, Richmond Hill, ON, Canada), respectively. Z-slices of 0.5-μm step were acquired using Volocity (Improvision) through the cells using a piezo z-stage (Applied Scientific Instrumentation, Eugene, OR) every 1 min over a period of

30 min. Quantification of fluorescent intensity was done using Volocity, version 5.0.0 (Improvision, Lexington, MA).

Lipid Extraction and Thin Layer Chromatography (TLC) for Fluorescent Substrates

To characterize incorporation of the fluorescent FA analogues into lipid classes, hepatocytes were incubated with OA/BSA containing the fluorescent FA as described above for indicated time (1 min–4 h). Cells were then washed with PBS and harvested into 1 ml of ice-cold PBS and immediately transferred to 4 ml of chloroform or neutral lipid solvent system to extract lipids. The lipid phase was collected and evaporated under N_2. Lipid residues were dissolved in 100 μl of chloroform applied onto silica gel H TLC plates (Whatmann, Florham Park, NJ). Separation of neutral lipids were performed by developing the plates in a neutral lipid solvent (heptane/isopropyl ether/acetic acid, 60:40:4, vol/vol/vol) (Lehner and Vance, 1999). The fluorescent FA incorporation into lipid classes was visualized under UV light (365 nm), and images were captured with a digital camera.

Metabolic Labeling of Lipids with [^{3}H]OA

Metabolic labeling was adapted from a method described previously (Wang *et al.*, 2007). In brief, WT and TGH KO hepatocytes were incubated for various time periods with serum-free DMEM containing 0.4 mM [^{3}H]OA (125 Ci/mol) complexed to 0.5% BSA. Cells were then washed, harvested, and disrupted by sonication. Microsomes were isolated by centrifugation at 99,000 × *g*, and lipids were extracted with chloroform/methanol (2:1, vol/vol) and resolved by TLC in the neutral lipid solvent. Radioactivity associated with TG, diacylglycerol (DG), and phospholipids (PL) was determined by scintillation counting.

Statistical Analysis

Unless otherwise stated, data are presented as means ± SD. Statistical significance was evaluated by two-tailed Student's *t* test.

RESULTS

TGH Is Localized in the ER Surrounding LDs

To address the potential interaction of TGH with cytosolic LDs, hepatocytes transfected with a cDNA encoding TGH-EGFP fusion protein were incubated with OA and subcellular localization of TGH-EGFP and LDs was observed by confocal microscopy. TGH-EGFP was excluded from the nucleus and assumed expected ER localization manifested in the reticular pattern throughout the cells (Figure 1A). TGH-EGFP also localized extensively to areas surrounding the cytosolic LDs (Figure 1A, right). The patchy distribution around the LDs is different from the typical ER localization, suggesting the possibility that TGH may preferentially localize to an ER area where the ER comes into contact with LDs. However, the resolution of confocal microscopy precludes the possibility to determine unequivocally whether TGH resides in the ER surrounding the LDs or whether it physically associates with LDs. Subcellular fractionation was performed to address this question. The results revealed that TGH predominantly cofractionated with the microsomal fraction together with the ER resident protein PDI and the ER polytopic membrane protein PEMT (Figure 1B). The LD fraction was enriched in the known LD coat protein ADRP (Figure 1B).

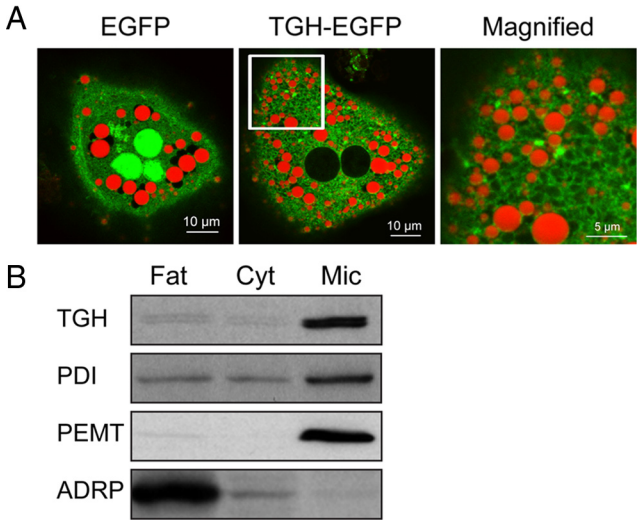

Figure 1. TGH is localized in the ER surrounding LDs. (A) Confocal images of hepatocytes transfected with plasmids encoding EGFP or TGH-EGFP. Green, EGFP; red, Nile Red (LDs). A close-up of the area within the white box is shown as Magnified. TGH is found in close proximity to LDs. Bar, 10 μm (EGFP and TGH-EGFP) and 5 μm (Magnified). (B) Endogenous TGH cofractionates predominantly with the ER. Subcellular fractions from mouse liver homogenates were obtained as described under *Materials and Methods*. Equal volume from each fraction was analyzed. Fat, fat cake; Cyt, cytosol; Mic, microsomes.

Ablation of TGH Leads to OA-mediated Cytosolic TG Accumulation in Hepatocytes

We have shown previously (Wang *et al.*, 2007) that ectopic expression of TGH in McA cells led to decreased cytosolic

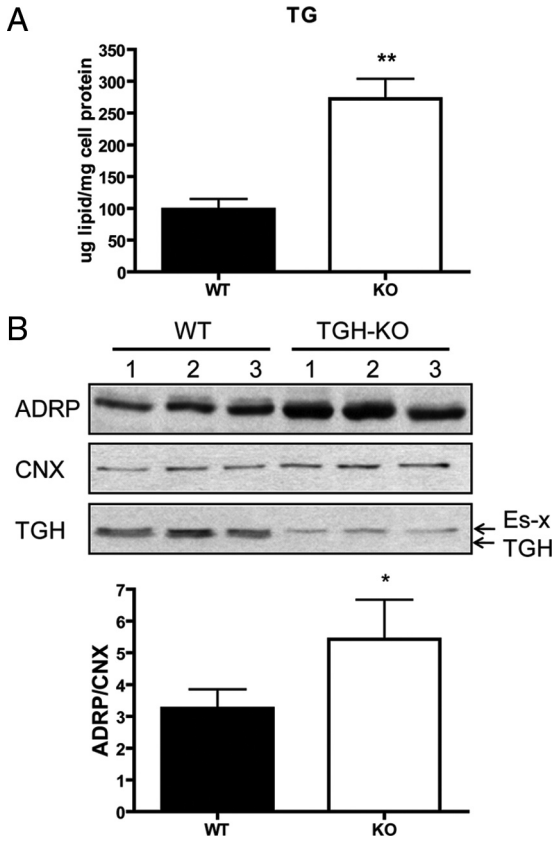

Figure 2. Ablation of TGH leads to TG accumulation in OA treated hepatocytes. WT and TGH KO hepatocytes were incubated overnight with DMEM containing 0.4 mM oleic acid complexed to 0.5% BSA. Three dishes of each cell type were analyzed. (A) Cytosol were isolated from cell homogenates, and TG mass was determined by gas chromatography. (B) Cell homogenates were analyzed for ADRP, calnexin (CNX), and TGH levels by Western blotting. Twenty micrograms of cell protein from cell homogenates was analyzed. ADRP levels were determined by densitometry and normalized to calnexin. Note that anti-TGH sera recognize both TGH (bottom band) and a protein highly homologous to TGH, Es-x (top band). *$p < 0.05$; **$p = 0.001$; NS, not significant.

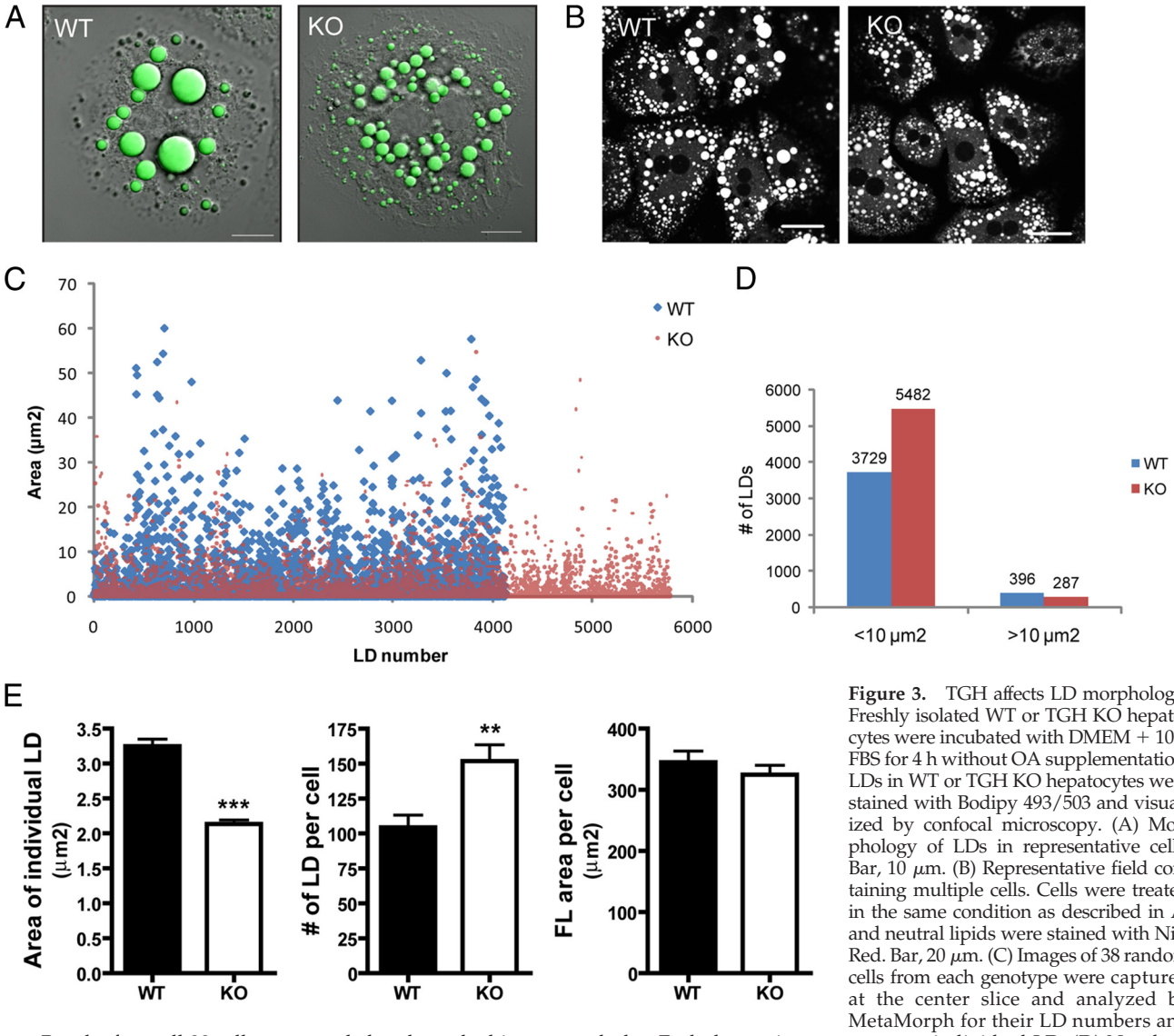

Figure 3. TGH affects LD morphology. Freshly isolated WT or TGH KO hepatocytes were incubated with DMEM + 10% FBS for 4 h without OA supplementation. LDs in WT or TGH KO hepatocytes were stained with Bodipy 493/503 and visualized by confocal microscopy. (A) Morphology of LDs in representative cells. Bar, 10 μm. (B) Representative field containing multiple cells. Cells were treated in the same condition as described in A, and neutral lipids were stained with Nile Red. Bar, 20 μm. (C) Images of 38 random cells from each genotype were captured at the center slice and analyzed by MetaMorph for their LD numbers and areas. Results from all 38 cells were pooled and graphed in scattered plot. Each data point represents an individual LD. (D) Numbers of LDs with areas $\leq$10 μm^2 or >10 μm^2 were counted and presented in bar graph. (E) Average area of an individual LD, number of LDs per cell, and total area of LDs per cell were quantified. **p = 0.001; ***p < 0.0001. Data are presented as means ± SEM.

TG accumulation, suggesting that TGH activity can either prevent cytosolic LD formation or increase their turnover. To address the role of TGH in cytosolic LD homeostasis, we used primary hepatocytes isolated from mice in which *Tgh* expression has been genetically ablated. Our working hypothesis was that lack of *Tgh* expression would increase OA-mediated TG accumulation in the cytosolic LDs. As expected, incubation of TGH-deficient (KO) hepatocytes with OA led to a 2.8-fold increase in the cytosolic TG levels compared with WT cells (Figure 2A). Correspondingly, a 1.7-fold increase in ADRP level also was observed (Figure 2B).

Ablation of TGH Alters the Morphology of LDs

Freshly isolated hepatocytes from fasted TGH-deficient mice contained LDs that were significantly smaller but more numerous compared with those in control (WT) cells (Figure 3, A and B). The size of LDs varies from below 0.01 μm^2 to up to 50 μm^2. Although the majority of LDs was below 10 μm^2 in both genotypes, WT cells contained more LDs larger than 10 μm^2 (Figure 3, C and D). TGH-deficient cells exhibited a 34% decrease in the average area of an individual LD, but 45% increase in LD number. As a result, total LD area (fluorescent area) was comparable with that in control cells (Figure 3E), indicating similar TG content. It is important to note that these results were obtained from freshly isolated hepatocytes from fasted mice without incubation with exogenous OA and that the results therefore reflect in vivo conditions, which are different from conditions used in Figure 2 in which isolated cells were incubated with exogenous OA to augment TG stores. The lack of accumulation of hepatic TG in TGH deficiency agrees with the proposed role of TGH in the mobilization of FA from adipose tissue (Soni *et al.*, 2004; Wei *et al.*, 2007b) and our recent studies indicating that hepatic TG levels in TGH-deficient mice were not statistically different from WT mice in fasted state due to decreased FA delivery to the liver from adipose tissue in the absence of TGH (Wei *et al.*, 2010).

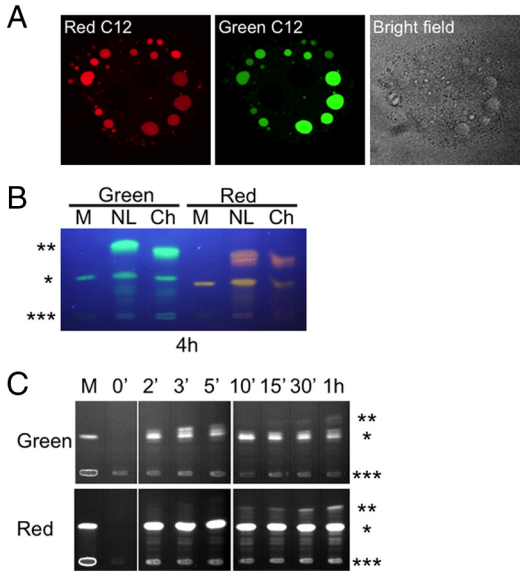

Figure 4. Characterization of Bodipy FA analogues. (A) WT hepatocytes were labeled with Green- and Red-C_{12} for 4 h, and incorporation into LDs were visualized by confocal microscopy. (B) Cells were labeled with Green or Red C_{12} for 4 h. Lipids were then extracted with chloroform (Ch) or neutral lipid solvent (NL) and lipid classes were resolved on TLC plates. (C) Time course of incorporation of Bodipy FA into glycerolipids. The migration of FA analogues and esterification products was visualized by excitation with UV-light. *, unesterified Bodipy FA analogues; **, analogues incorporated into neutral lipids; ***, analogues incorporated into phospholipids; M, media containing unesterified Bodipy FA before addition to cells.

TGH Deficiency Does Not Alter the Formation of Nascent LDs

LDs are dynamic intracellular bodies that are initially formed as nascent particles probably at the site of TG synthesis on the ER. This is followed by expansion through additional transfer of lipids into the preformed LDs and finally lipolysis of LD-associated TG for energy production and other cellular events. Because we have demonstrated previously that TGH is involved in hepatic TG metabolism (Lehner and Vance, 1999; Gilham *et al*., 2003; Wang *et al*., 2007; Wei *et al*., 2007a) and that TGH is localized to the ER where TG synthesis and therefore biogenesis of LDs occurs (Lehner *et al*., 1999; Gilham *et al*., 2005; Wang *et al*., 2007), we rationalized that TGH activity might regulate LD dynamics. We wanted to first address whether TGH plays a role in the nascent LD formation. To this end, we introduced fluorescent FA analogues as tracers for TG synthesis and the integration of TG into LDs. The two FA analogues used were Bodipy 558/568 C_{12} (referred to as Red C_{12} hereafter) and Bodipy FL C_{12} (referred to as Green C_{12}). Both Red C_{12} and Green C_{12} can be integrated into LDs with similar distribution (Figure 4A).

To further examine whether the FA analogues were incorporated into LDs in their esterified form, neutral lipids from cells labeled with these fluorescent FA analogues were isolated and the lipid classes were resolved by TLC (Figure 4B, left). Due to a different polarity between the Bodipy FA and natural FA, free Bodipy FA migrated with slower mobility in the neutral lipid solvent system compared with OA (data not shown). The Bodipy FA was incorporated into both glycerophospholipids (fluorescence at the origin) and neutral lipids that migrated with faster mobility than the free Bodipy FA, consistent with TG and cholesteryl ester migration in this system (Figure 4B). A study wherein cells were labeled with the Bodipy FA for variable periods revealed that although significant amount of free Bodipy FA was detected (which may represent cell surface-associated FA), some of the Bodipy FA was incorporated into neutral lipids gradually with time (Figure 4C, **), whereas incorporation of the Bodipy FA into polar lipids seemed to occur rapidly (Figure 4C, ***). Fluorescent microscopy experiments also demonstrated that the Bodipy FA entered the hydrophobic core of LDs (Figures 4A and 7C), a process that requires an esterified, nonpolar molecule.

To study LD dynamics, cells were first incubated with Green C_{12} supplemented with OA/BSA overnight to represent preformed LDs (Figure 5A, green globules). Cells were then incubated for 15 min with Red C_{12}/OA/BSA to label newly formed LDs. At the end of 15 min, Red C_{12} distributed mainly within the ER, manifested as red reticular structures (Figure 5A). This reticular structure coincided with the area of the ER where TGH was localized (Figure 5B). Distribution of newly synthesized lipids in the ER may be due to initial incorporation of FA into membrane PL. Alternatively, it also could be due to accumulation of nascent LDs within the ER bilayer or in the ER lumen. Most preformed LDs were apposed to these red-fluorescing ER structures (Figure 5A). Small, nascent LDs were seen to emerge from discrete areas of the ER. We compared nascent LD formation between WT and KO cells. Similar amount of nascent LDs with diameters ranging from 0.2 to 0.6 μm were observed in both genotypes (Figure 5C), indicating that the absence of TGH did not affect nascent LD formation. A few of these nascent LDs colocalized with small, preformed LDs (Figure 5A), suggesting ongoing merging events between these two types of LDs. However, the majority of LDs remained unmixed after 15-min incubation.

We intended to elucidate whether these nascent LDs were associated with any known LD-coat proteins. WT hepatocytes were incubated with Red C_{12} for 15 min, followed by immunofluorescent staining for two LD-coat proteins ADRP and TIP47. Although it is not possible to prevent labeled lipids from entering preformed LDs during immunostaining because lipids cannot be fixed by formaldehyde or glutaraldehyde and may diffuse between LDs once cells are permeabilized, the majority of nascent LDs were distinguishable from preformed LDs that were lightly stained. The results demonstrated that numerous Red C_{12}-containing nascent LDs were associated with TIP47, but not with ADRP, whereas ADRP was localized mainly on the surface of preformed LDs (Figure 5D). The partial colocalization of nascent LDs with TIP47 suggests the early stage of LD formation and commencement of LD-coat protein recruitment. These results are consistent with previous observations in 3T3-L1 cells where TIP47 was localized on the smallest, newly formed LDs, whereas ADRP was mainly present on larger LDs (Wolins *et al*., 2005, 2006).

TGH Deficiency Delays LD Maturation

Differences between LD dynamics in WT and TGH KO hepatocytes were revealed during investigation of the time course of incorporation of Red C_{12}-labeled lipids into preexisting LDs. In WT cells, some preformed LDs were seen to colocalize with nascent LDs at 30 min, suggesting the transfer of newly synthesized TG to preformed LDs at this stage (Figure 6A). In contrast, no apparent lipid transfer was observed in KO hepatocytes until 1 h of incubation (Figure 6A). These results suggested delayed transfer of newly synthesized lipids into preformed LDs in the absence of TGH. However, the process is

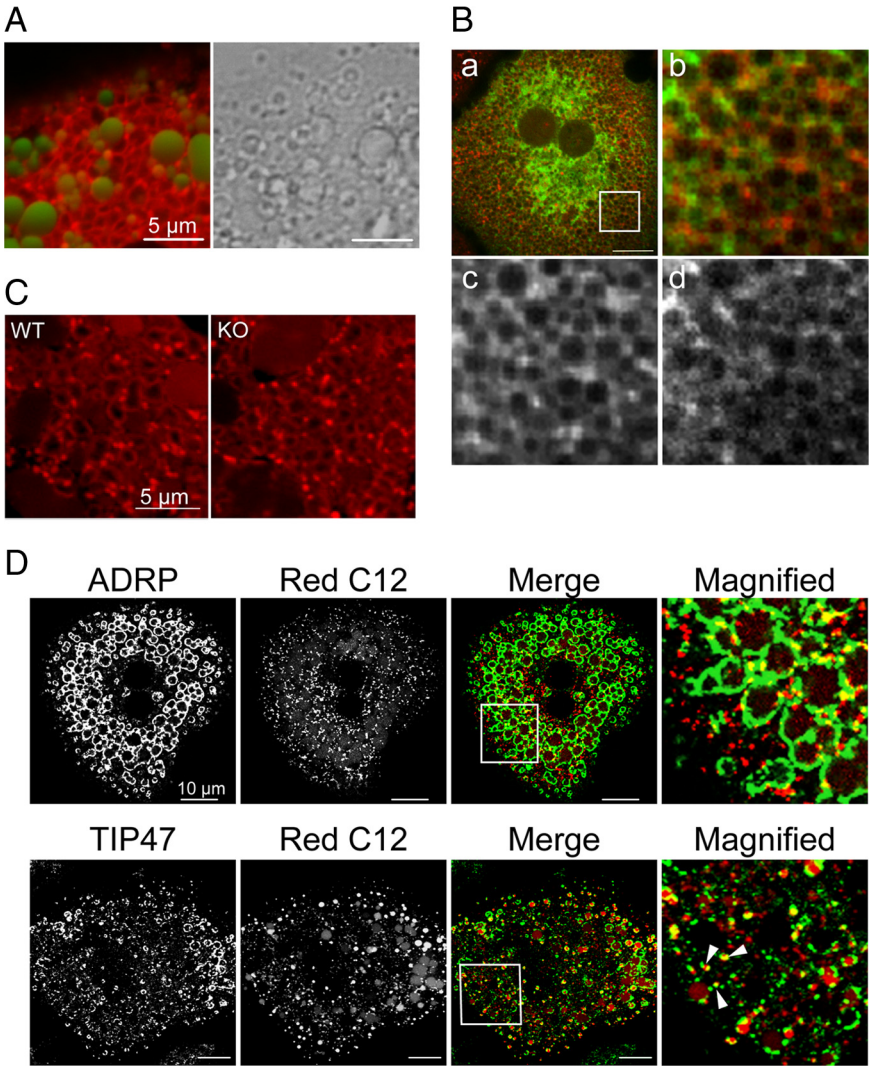

Figure 5. TGH does not affect nascent LD formation. (A) Cells were labeled with Bodipy FL C_{12} overnight (preformed LDs; green), followed by Bodipy 558/568 C_{12} for 15 min (nascent LDs; red). Nascent LDs emerge at discrete ER locations surrounding the preformed LDs. (B) TGH deficient hepatocytes were transfected with TGH-EGFP and fluorescently labeled with Red C_{12} for 15 min. The colocalization of TGH-EGFP and integration of Red C_{12} was determined by confocal microscopy. A representative cell is presented (a). The area in the white box is magnified (b). (c) Red C_{12}. (d) TGH-EGFP. Bar, 10 μm. (C) Formation of nascent LDs in WT and TGH KO cells at 15 min is similar. (D) Nascent LDs extensively associate with TIP47 but not ADRP. WT hepatocytes were incubated with OA/BSA overnight. Nascent LDs were then labeled with Red C_{12} for 15 min and immunostained for ADRP and TIP47 as described in *Materials and Methods*. Arrowhead, association of TIP47 with surface of nascent LDs.

only delayed rather than abolished, because after 4-h incubation, essentially all preformed LDs have incorporated newly synthesized lipids in the presence or absence of TGH. Therefore, TGH seems to affect the rate of lipid transfer into preformed LDs. This phenomenon can be seen more clearly in live-cell imaging (Figure 6B and Supplemental Video S1). In the supplemental video, Red C_{12} globules represent preformed LDs and Green C_{12} labels nascent LDs. The preformed LDs were relatively static, whereas the nascent LDs were highly dynamic. In WT cells, nascent lipids were integrated into the preformed LDs rapidly and extensively, whereas in TGH-deficient cells, the incorporation was only seen in a few LDs. The amount of newly synthesized lipids that became incorporated into preformed LDs over time was quantified (Figure 6C). The signal intensity of preformed lipids (Red C_{12}) remained relatively stable in both WT and KO cells during the 30-min incubation. However, the curve for incorporation of newly synthesized lipids into preexisting LDs was much steeper in WT cells than that in KO cells, with threefold increase in WT cells at the end of 30-min incubation compared with only 50% increase in KO cells (Figure 6C), indicating that in the presence of TGH, preformed LDs obtain newly synthesized lipids much faster than when this lipase is absent. These results strongly suggest a positive role for TGH in LD maturation.

Ablation of TGH Expression Results in the Accumulation of DG and PL in the Microsomes

Some intermediates in lipid metabolism, especially DG, have been implicated in LD formation (Kuerschner *et al*., 2008) and the recruitment of LD-coat proteins (Skinner *et al*., 2009). To investigate the potential mechanism by which TGH may regulate LD maturation, we examined lipid synthesis in WT and TGH KO cells by metabolic labeling with exogenously supplied OA. The rate of TG synthesis in the microsomes did not differ in WT and TGH KO hepatocytes; however, the KO cells presented with a marked increase in microsomal DG at all time points. Increased formation of DG was accompanied by elevated PL levels in TGH KO cells (Figure 6D).

Nascent LDs Interact with Preformed LDs Dynamically

Fusion between LDs is generally thought to be an important mechanism for LD growth (Fujimoto *et al*., 2008; Goodman, 2008; Olofsson *et al*., 2008). We attempted to address whether fusion between nascent and preformed LDs oc-

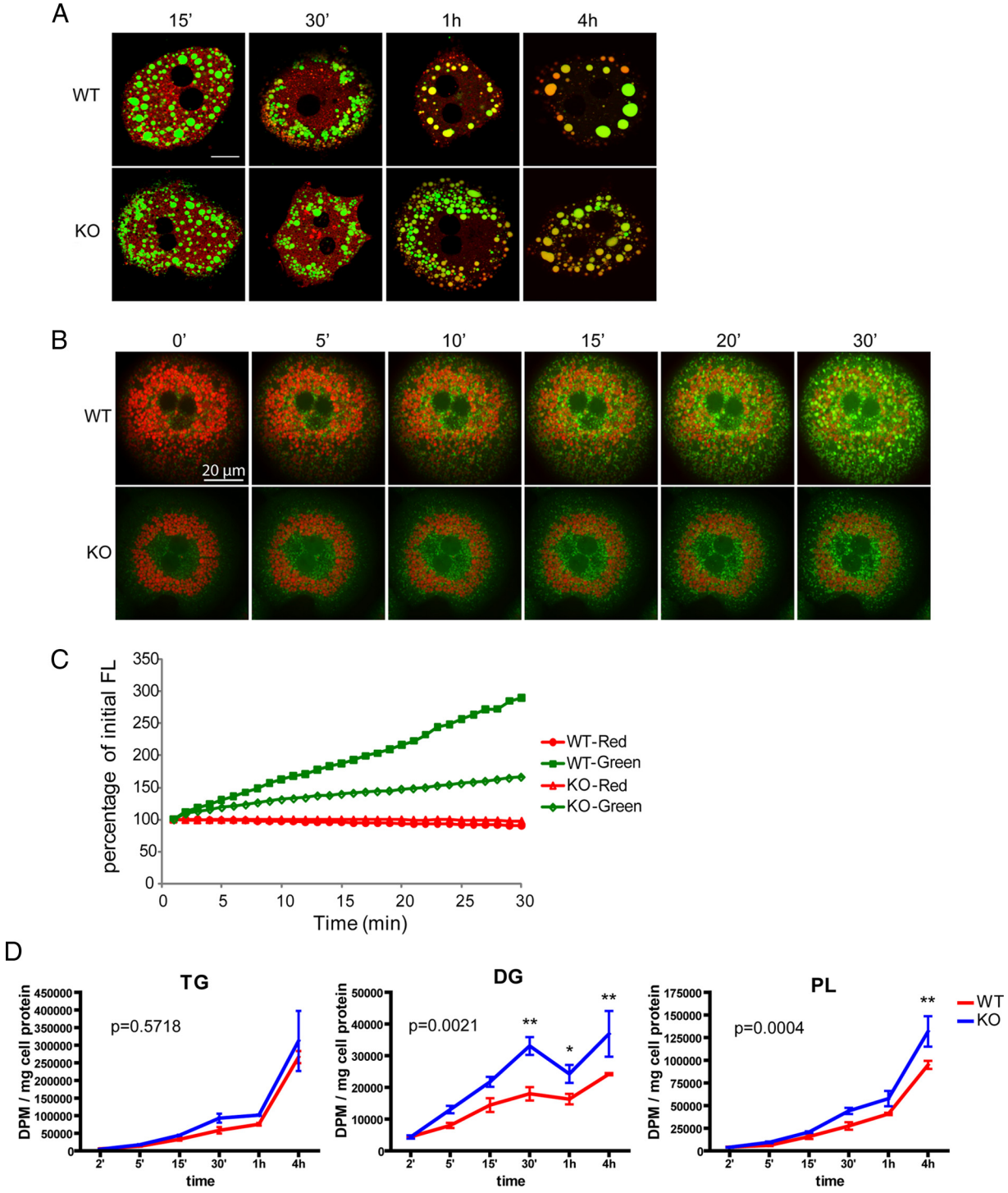

Figure 6. TGH deficiency delays the merge of nascent and preformed LDs. (A) WT and TGH KO hepatocytes were labeled with labeling media containing Green C_{12} overnight, followed by incubation with Red C_{12}-containing labeling media for indicated periods. Cells were then fixed and mounted onto coverslips. Confocal images were captured and representative cells are presented. Bar, 10 μm. (B) Live imaging of LD formation. WT and TGH KO hepatocytes were labeled with Red C_{12}-containing media overnight, and fatty acid uptake reagent (containing Green C_{12}) was added immediately before the start of image acquisition (0 min) with time-lapse confocal microscopy. Image stacks were taken every 1 min for 30 min. Images at indicated times were presented at extended focus mode. The corresponding videos were shown in Supplemental Video S1, A and B. Data presented in this figure is a representative of three to five cells obtained during each experiment for four repeated experiments. (C) Images at all time points were analyzed for fluorescent intensity. Areas of analysis were defined by the signal intensity obtained with the Cy3 channel (red) within a certain threshold, representing the area occupied by the preformed LDs. The same threshold was set for WT and TGH KO cells. Fluorescent intensities of Cy3 (red) and GFP (green) channels within the defined areas at each time point were quantified. Fluorescent intensity at each time point is presented as percentage of initial fluorescence (0 min). (D) DG and PL accumulation in TGH KO hepatocytes. Cells were incubated with [^{3}H]OA as described in *Materials and Methods* and analyzed for incorporation of radioactivity into microsomal TG, DG, and PL at indicated times. Statistical analysis of differences between WT and KO at all times from triplicate experiments were evaluated by two-way analysis of variance. *$p < 0.05$; **$p < 0.01$.

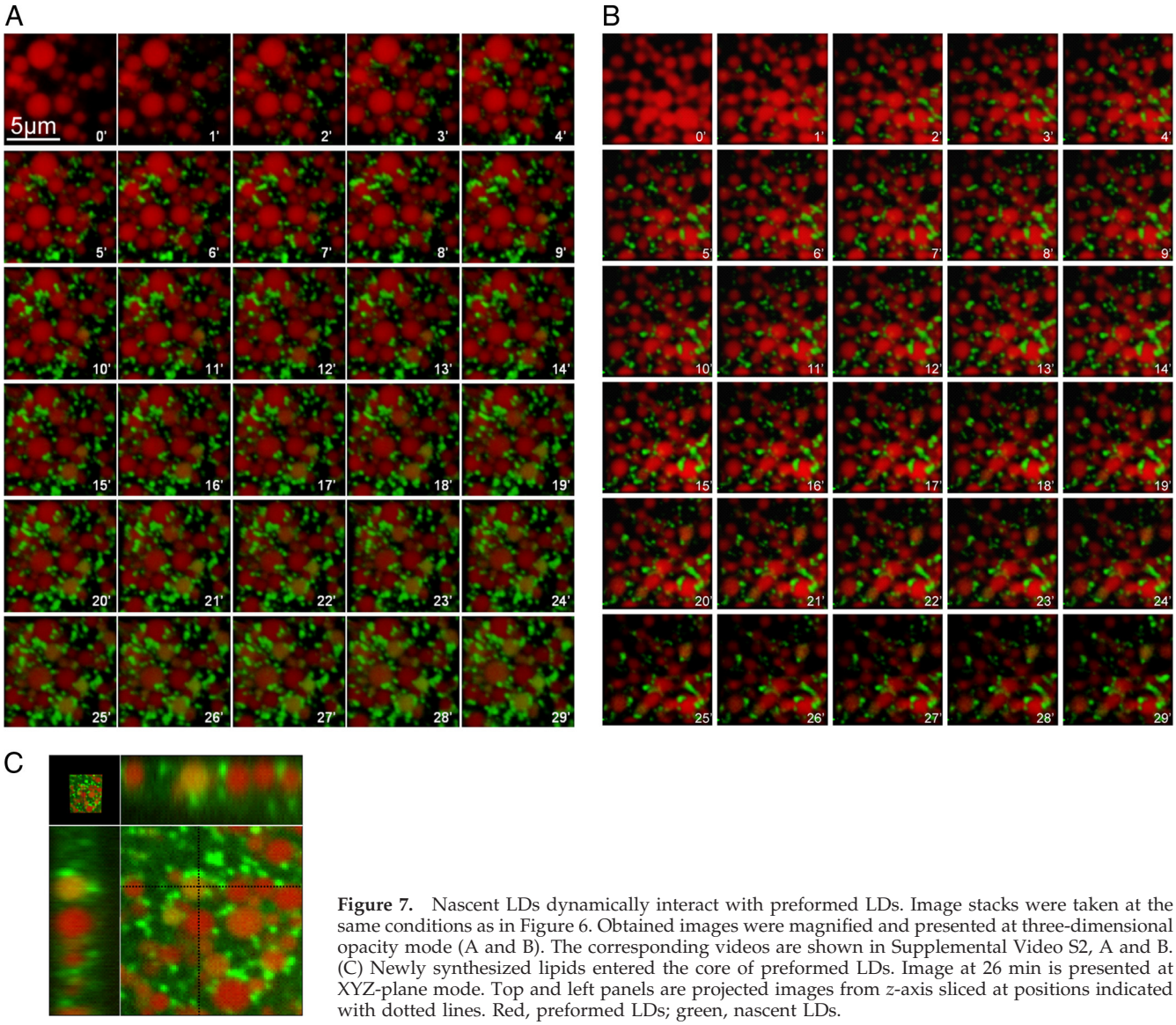

Figure 7. Nascent LDs dynamically interact with preformed LDs. Image stacks were taken at the same conditions as in Figure 6. Obtained images were magnified and presented at three-dimensional opacity mode (A and B). The corresponding videos are shown in Supplemental Video S2, A and B. (C) Newly synthesized lipids entered the core of preformed LDs. Image at 26 min is presented at XYZ-plane mode. Top and left panels are projected images from *z*-axis sliced at positions indicated with dotted lines. Red, preformed LDs; green, nascent LDs.

curred and served as a mechanism for the transfer of lipids from nascent to preformed LDs in primary hepatocytes. Live-cell images of WT and TGH-deficient hepatocytes were taken at the same resolution and magnified after image capture to analyze LD interactions (Figure 7, A and B, and Supplemental Videos S2, A and B). In WT cells, nascent LDs rapidly formed around and dynamically interacted with preformed LDs. These brief interactions seemed to lead to the transfer of newly synthesized lipids from nascent LDs into the core of preformed LDs (Figure 7C). However, no apparent fusion was observed between nascent and preformed LDs, at least within the 30-min duration the movie represents. Transfer of lipids seemed to follow a gradual process rather than "bulk" lipidation. These results indicate that if fusion were used in the growth of hepatic LDs, it seems to be a series of dynamic, transient fusions instead of full-collapse fusions. In TGH-deficient cells, the dynamic movement of nascent LDs and their interaction with preformed LDs remained intact (Figure 7B and Supplemental Video S2B), indicating this process may be independent of TGH activity.

DISCUSSION

We report that TGH, in addition to being a key enzyme in hepatic VLDL assembly, also regulates LD maturation in hepatocytes. This is the first time an ER luminal lipase has been reported to regulate metabolism of cytosolic LDs. Our results indicate that TGH localizes in areas of ER proximal to cytosolic LDs.

Two fluorescent Bodipy FA analogues were used in our studies to address the dynamics of LD formation. One of the main concerns in using these analogues is their metabolic behavior compared with natural FA. Incorporation of Bodipy FA analogues into TG, DG, and phosphatidylcholine (PC) has been demonstrated to occur in baby hamster kidney cells (Kasurinen, 1992). Both Bodipy FL C_{12} and Bodipy 558/568 C_{12} have been used in studies to trace LD formation in adipocytes and hepatoma cell lines (Targett-Adams *et al*., 2003; Wolins *et al*., 2005; Turro *et al*., 2006). To further address the metabolic behavior of the Bodipy FA analogues in hepatocytes, we assessed their incorporation into various lipid classes. Bodipy FA were esterified into neutral lipids, and these lipids were incor-

porated into the core of LDs. In addition, small globular structures formed after labeling with Red C_{12} for 15 min were found extensively associated with the LD-coat protein TIP47, suggesting they are bona fide LDs. Therefore, we concluded that Bodipy FA analogues were suitable substrates to trace LD formation.

We intended to investigate the formation and turnover of TG containing LDs in hepatocytes supplied with FA. We observed that nascent LDs with a diameter ranging from 0.2 to 0.6 μm rapidly formed from discrete areas of the ER (Figure 5, A and B). It is generally accepted that the ER is the birthplace of LDs, but the mechanism by which LDs accrue additional lipids and grow in size remains speculative. In their recent review, Walther and Farese (2009) proposed two possible mechanisms for LD maturation. The first possibility involves diffusion of lipids formed in the ER into ER-associated LDs. The second possibility involves addition of lipids to LDs after their detachment from the ER. Many studies have found resident ER proteins (in certain instances even transmembrane proteins) in LD preparations, which would seem to support the first hypothesis. Studies in yeast have suggested that 92–97% of LDs remain associated with the ER (Szymanski *et al*., 2007). However, several lines of evidence also support the possibility that LDs may detach from the ER under certain conditions. It was demonstrated that in *Drosophila* (Welte *et al*., 1998) and in NIH-3T3 cells (Bostrom *et al*., 2005), LDs travel long distances along microtubules. In 3T3-L1 adipocytes, LDs also were shown to undergo dynamic remodeling during stimulated lipolysis (Brasaemle *et al*., 2004; Marcinkiewicz *et al*., 2006; Yamaguchi *et al*., 2007). These studies suggest cell-specific LD dynamics. If LDs indeed separate from the ER after birth, lipids would either need to be synthesized locally on the surface of LDs or a transfer protein would be required to carry lipids from the site of synthesis (the ER) to LDs for LDs to grow in size, or LDs would grow in size by fusion.

Homotypic fusion events between LDs have been observed by time-lapse microscopy in oleic acid treated NIH 3T3 cells (Bostrom *et al*., 2005). However, the observation could not exclude the possibility that the LDs that underwent fusion separate again (fission) immediately after the observed fusion. The most convincing evidence to support fusion has been reported recently by Bostrom *et al*. (2007). By knocking down the soluble *N*-ethylmaleimide-sensitive factor attachment protein receptors (SNAREs), proteins that mediate vesicle fusion, it was shown that SNAREs are essential for LD fusion and growth in NIH-3T3 cells. The fusion events did not seem to be regulated by TG synthesis in these cells.

In our research, we did not observe apparent fusion events in primary mouse hepatocytes. This is possibly because fusion was a transient and rare event that may occur much faster than the time interval between image acquisitions during time-lapse microscopy. Alternatively, fusions may take place at much later stages of LD maturation, i.e., after the initial 30 min we analyzed. Instead of a full-collapse fusion, data from the time-lapse microscopy (Figure 7 and Supplemental Video S2) suggested a dynamic interaction and gradual lipid transfer between nascent and preformed LDs. It is possible that a transient fusion and fission occurred during the contact between the two participating LDs, leading to the transfer of content from nascent to performed LDs. It is currently unknown why lipids only seemed to transfer from nascent to preformed LDs but not in the other direction. This phenomenon might be due to the different composition of surface components in ADRP-containing large LDs compared with TIP47-containing small LDs. Preformed, ADRP-containing LDs may represent a relatively inert pool for long-term TG storage, as evidenced by the relatively constant Red C_{12} intensity in both cell types (Figure 6C). On the contrary, the nascent, TIP47-containing LDs may represent metabolically active pool that undergoes dynamic formation and breakdown. TGH deficiency delayed the lipid transfer from the nascent to preformed LDs, suggesting a role of TGH in maintaining the homeostasis of the inert and active pool of TG.

To address the potential mechanism by which lack of TGH expression alters LD morphology and dynamics, we performed metabolic labeling of hepatocytes with radiolabeled OA and followed a time course of lipid synthesis. TGH deficiency was accompanied by accumulation of microsomal DG and PL. The accumulation of DG in the microsomes in the absence of TGH is probably due to deficiency in TGH-mediated lipolysis of neutral lipids, reminiscent of HSL deficiency in the adipose tissue (Haemmerle *et al*., 2002), and might indicate greater specific activity of TGH toward DG than TG. Previous studies have suggested that TGH possesses a DG lipase activity and it hydrolyzes DG more efficiently than TG in the in vitro system (Lehner and Verger, 1997). Increased DG levels in the ER is known to result in the recruitment of CTP:phosphocholine cytidylyltransferase (CT) from its cytosolic catalytically inert pool to catalytically active membrane-associated pool leading to augmented PC synthesis (Jamil *et al*., 1993). Increased PC to core lipids ratio results in increased surface area of LDs and reduced LD size. In support of the role of PC in regulating LD size, it has been observed in *Drosophila* S2 cells that CT-deficient cells have larger LDs that were hypothesized to be formed due to either a failure to form new LDs, or the compromised fusion of LDs (Guo *et al*., 2008). Accordingly, genetic ablation of hepatic CTα expression also resulted in the formation of large LDs (Jacobs *et al*., 2004; Jacobs *et al*., 2008). Therefore, increased PC synthesis observed in TGH-deficient hepatocytes would be expected to result in smaller LDs and the LDs would be less likely to undergo coalescence/fusion and thus delayed maturation would ensue.

ACKNOWLEDGMENTS

We thank Honey Chan for help in confocal fluorescent scanning microscopy and Randy Nelson for help in hepatocyte transfection. We also thank Johanne Lamoureux and Lena Li for the generous technical assistance. This research was supported by Canadian Institute of Health Research grant MOP 69043. H. W. is supported by the Heart and Stoke Foundation of Canada doctoral research award and by the Alberta Heritage Foundation for Medical Research full-time studentship award. N. T. is a scholar and R. L. is a senior scholar of the Alberta Heritage Foundation for Medical Research.

REFERENCES

Bostrom, P., *et al*. (2007). SNARE proteins mediate fusion between cytosolic lipid droplets and are implicated in insulin sensitivity. Nat. Cell Biol. *9*, 1286–1293.

Bostrom, P., Rutberg, M., Ericsson, J., Holmdahl, P., Andersson, L., Frohman, M. A., Boren, J., and Olofsson, S. O. (2005). Cytosolic lipid droplets increase in size by microtubule-dependent complex formation. Arterioscler. Thromb. Vasc. Biol. *25*, 1945–1951.

Brasaemle, D. L. (2007). Thematic review series: adipocyte biology. The perilipin family of structural lipid droplet proteins: stabilization of lipid droplets and control of lipolysis. J. Lipid Res. *48*, 2547–2559.

Brasaemle, D. L., Dolios, G., Shapiro, L., and Wang, R. (2004). Proteomic analysis of proteins associated with lipid droplets of basal and lipolytically stimulated 3T3-L1 adipocytes. J. Biol. Chem. *279*, 46835–46842.

Dolinsky, V. W., Gilham, D., Alam, M., Vance, D. E., and Lehner, R. (2004). Triacylglycerol hydrolase: role in intracellular lipid metabolism. Cell. Mol. Life Sci. *61*, 1633–1651.

Fujimoto, T., Ohsaki, Y., Cheng, J., Suzuki, M., and Shinohara, Y. (2008). Lipid droplets: a classic organelle with new outfits. Histochem. Cell Biol. *130*, 263–279.

Gibbons, G. F., Islam, K., and Pease, R. J. (2000). Mobilisation of triacylglycerol stores. Biochim. Biophys. Acta *1483*, 37–57.

Gibbons, G. F., and Wiggins, D. (1995). Intracellular triacylglycerol lipase: its role in the assembly of hepatic very-low-density lipoprotein (VLDL). Adv. Enzyme Regul. *35*, 179–198.

Gilham, D., Alam, M., Gao, W., Vance, D. E., and Lehner, R. (2005). Triacylglycerol hydrolase is localized to the endoplasmic reticulum by an unusual retrieval sequence where it participates in VLDL assembly without utilizing VLDL lipids as substrates. Mol. Biol. Cell *16*, 984–996.

Gilham, D., Ho, S., Rasouli, M., Martres, P., Vance, D. E., and Lehner, R. (2003). Inhibitors of hepatic microsomal triacylglycerol hydrolase decrease very low density lipoprotein secretion. FASEB J. *17*, 1685–1687.

Gilham, D., and Lehner, R. (2004). The physiological role of triacylglycerol hydrolase in lipid metabolism. Rev. Edocr. Metab. Disord. *5*, 303–309.

Goodman, J. M. (2008). The gregarious lipid droplet. J. Biol. Chem. *283*, 28005–28009.

Guo, Y., Walther, T. C., Rao, M., Stuurman, N., Goshima, G., Terayama, K., Wong, J. S., Vale, R. D., Walter, P., and Farese, R. V. (2008). Functional genomic screen reveals genes involved in lipid-droplet formation and utilization. Nature *453*, 657–661.

Haemmerle, G., Zimmermann, R., Hayn, M., Theussl, C., Waeg, G., Wagner, E., Sattler, W., Magin, T. M., Wagner, E. F., and Zechner, R. (2002). Hormone-sensitive lipase deficiency in mice causes diglyceride accumulation in adipose tissue, muscle, and testis. J. Biol. Chem. *277*, 4806–4815.

Holm, C., Belfrage, P., and Fredrikson, G. (1987). Immunological evidence for the presence of hormone-sensitive lipase in rat tissues other than adipose tissue. Biochm. Biophys. Res. Commun. *148*, 99–105.

Jacobs, R. L., Devlin, C., Tabas, I., and Vance, D. E. (2004). Targeted deletion of hepatic CTP:phosphocholine cytidylyltransferase alpha in mice decreases plasma high density and very low density lipoproteins. J. Biol. Chem. *279*, 47402–47410.

Jacobs, R. L., Lingrell, S., Zhao, Y., Francis, G. A., and Vance, D. E. (2008). Hepatic CTP:phosphocholine cytidylyltransferase-alpha is a critical predictor of plasma high density lipoprotein and very low density lipoprotein. J. Biol. Chem. *283*, 2147–2155.

Jamil, H., Hatch, G. M., and Vance, D. E. (1993). Evidence that binding of CTP:phosphocholine cytidylyltransferase to membranes in rat hepatocytes is modulated by the ratio of bilayer- to non-bilayer-forming lipids. Biochem. J. *291*, 419–427.

Kasurinen, J. (1992). A novel fluorescent fatty acid, 5-methyl-BDY-3-dodecanoic acid, is a potential probe in lipid transport studies by incorporating selectively to lipid classes of BHK cells. Biochem. Biophys. Res. Commun. *187*, 1594–1601.

Kuerschner, L., Moessinger, C., and Thiele, C. (2008). Imaging of lipid biosynthesis: how a neutral lipid enters lipid droplets. Traffic *9*, 338–352.

Lankester, D. L., Brown, A. M., and Zammit, V. A. (1998). Use of cytosolic triacylglycerol hydrolysis products and of exogenous fatty acid for the synthesis of triacylglycerol secreted by cultured rat hepatocytes. J. Lipid Res. *39*, 1889–1895.

Lehner, R., Cui, Z., and Vance, D. E. (1999). Subcellullar localization, developmental expression and characterization of a liver triacylglycerol hydrolase. Biochem. J. *338*, 761–768.

Lehner, R., and Vance, D. E. (1999). Cloning and expression of a cDNA encoding a hepatic microsomal lipase that mobilizes stored triacylglycerol. Biochem. J. *343*, 1–10.

Lehner, R., and Verger, R. (1997). Purification and characterization of a porcine liver microsomal triacylglycerol hydrolase. Biochemistry *36*, 1861–1868.

Marcinkiewicz, A., Gauthier, D., Garcia, A., and Brasaemle, D. L. (2006). The phosphorylation of serine 492 of perilipin a directs lipid droplet fragmentation and dispersion. J. Biol. Chem. *281*, 11901–11909.

Martin, S., and Parton, R. G. (2006). Lipid droplets: a unified view of a dynamic organelle. Nat. Rev. *7*, 373–378.

Murphy, D. J., and Vance, J. (1999). Mechanisms of lipid-body formation. Trends Biochem. Sci. *24*, 109–115.

Olofsson, S. O., Bostrom, P., Andersson, L., Rutberg, M., Perman, J., and Boren, J. (2008). Lipid droplets as dynamic organelles connecting storage and efflux of lipids. Biochim. Biophys. Acta *1791*, 448–458.

Olofsson, S. O., Stillemark-Billton, P., and Asp, L. (2000). Intracellular assembly of VLDL: two major steps in separate cell compartments. Trends Cardiovasc. Med. *10*, 338–345.

Reid, B. N., Ables, G. P., Otlivanchik, O. A., Schoiswohl, G., Zechner, R., Blaner, W. S., Goldberg, I. J., Schwabe, R. F., Chua, S. C., Jr., and Huang, L. S. (2008). Hepatic overexpression of hormone-sensitive lipase and adipose triglyceride lipase promotes fatty acid oxidation, stimulates direct release of free fatty acids, and ameliorates steatosis. J. Biol. Chem. *283*, 13087–13099.

Shelness, G. S., and Sellers, J. A. (2001). Very-low-density lipoprotein assembly and secretion. Curr. Opin. Lipidol. *12*, 151–157.

Skinner, J. R., Shew, T. M., Schwartz, D. M., Tzekov, A., Lepus, C. M., Abumrad, N. A., and Wolins, N. E. (2009). Diacylglycerol enrichment of endoplasmic reticulum or lipid droplets recruits perilipin 3/TIP47 during lipid storage and mobilization. J. Biol. Chem. *284*, 30941–30948.

Soni, K. G., Lehner, R., Metalnikov, P., O'Donnell, P., Semache, M., Gao, W., Ashman, K., Pshezhetsky, A. V., and Mitchell, G. A. (2004). Carboxylesterase 3 (EC 3.1.1.1) is a major adipocyte lipase. J. Biol. Chem. *279*, 40683–40689.

Szymanski, K. M., Binns, D., Bartz, R., Grishin, N. V., Li, W. P., Agarwal, A. K., Garg, A., Anderson, R. G., and Goodman, J. M. (2007). The lipodystrophy protein seipin is found at endoplasmic reticulum lipid droplet junctions and is important for droplet morphology. Proc. Natl. Acad. Sci. USA *104*, 20890–20895.

Targett-Adams, P., Chambers, D., Gledhill, S., Hope, R. G., Coy, J. F., Girod, A., and McLauchlan, J. (2003). Live cell analysis and targeting of the lipid droplet-binding adipocyte differentiation-related protein. J. Biol. Chem. *278*, 15998–16007.

Turro, S., Ingelmo-Torres, M., Estanyol, J. M., Tebar, F., Fernandez, M. A., Albor, C. V., Gaus, K., Grewal, T., Enrich, C., and Pol, A. (2006). Identification and characterization of associated with lipid droplet protein 1, a novel membrane-associated protein that resides on hepatic lipid droplets. Traffic *7*, 1254–1269.

Walther, T. C., and Farese, R. V., Jr. (2009). The life of lipid droplets. Biochim. Biophys. Acta *1791*, 459–466.

Wang, H., Gilham, D., and Lehner, R. (2007). Proteomic and lipid characterization of apolipoprotein B-free luminal lipid droplets from mouse liver microsomes: implications for very low density lipoprotein assembly. J. Biol. Chem. *282*, 33218–33226.

Wei, E., Alam, M., Sun, F., Agellon, L. B., Vance, D. E., and Lehner, R. (2007a). Apolipoprotein B and triacylglycerol secretion in human triacylglycerol hydrolase transgenic mice. J. Lipid Res. *48*, 2597–2606.

Wei, E., Ben Ali, Y., Lyon, J., Wang, H., Nelson, R., Dolinsky, V. W., Dyck, J. R., Mitchell, G., Korbutt, G. S., and Lehner, R. (2010). Loss of TGH/Ces3 in mice decreases blood lipids, improves glucose tolerance, and increases energy expenditure. Cell Metabol. *11*, 183–193.

Wei, E., Gao, W., and Lehner, R. (2007b). Attenuation of adipocyte triacylglycerol hydrolase activity decreases basal fatty acid efflux. J. Biol. Chem. *282*, 8027–8035.

Welte, M. A., Gross, S. P., Postner, M., Block, S. M., and Wieschaus, E. F. (1998). Developmental regulation of vesicle transport in *Drosophila* embryos: forces and kinetics. Cell *92*, 547–557.

Wiggins, D., and Gibbons, G. F. (1992). The lipolysis/esterification cycle of hepatic triacylglycerol. Its role in the secretion of very-low-density lipoprotein and its response to hormones and sulphonylureas. Biochem. J. *284*, 457–462.

Wolins, N. E., Brasaemle, D. L., and Bickel, P. E. (2006). A proposed model of fat packaging by exchangeable lipid droplet proteins. FEBS Lett. *580*, 5484–5491.

Wolins, N. E., Quaynor, B. K., Skinner, J. R., Schoenfish, M. J., Tzekov, A., and Bickel, P. E. (2005). S3–12, Adipophilin, and TIP47 package lipid in adipocytes. J. Biol. Chem. *280*, 19146–19155.

Yamaguchi, T., Omatsu, N., Morimoto, E., Nakashima, H., Ueno, K., Tanaka, T., Satouchi, K., Hirose, F., and Osumi, T. (2007). CGI-58 facilitates lipolysis on lipid droplets but is not involved in the vesiculation of lipid droplets caused by hormonal stimulation. J. Lipd Res. *48*, 1078–1089.

Yang, L. Y., Kuksis, A., Myher, J. J., and Steiner, G. (1996). Contribution of de novo fatty acid synthesis to very low density lipoprotein triacylglycerols: evidence from mass isotopomer distribution analysis of fatty acids synthesized from [2H6]ethanol. J. Lipid Res. *37*, 262–274.

Zimmermann, R., *et al*. (2004). Fat mobilization in adipose tissue is promoted by adipose triglyceride lipase. Science *306*, 1383–1386.